Dynamic properties of water/alcohol mixtures studied by computer simulation

Erik J. W. Wensink and Alex C. Hoffmann
Department of Physics, University of Bergen, Allégatan 55, N-5007, Bergen, Norway

Paul J. van Maaren and David van der Spoel[a)]
Department of Cell and Molecular Biology, Uppsala University, Husargatan 3, Box 596, SE-751 24 Uppsala, Sweden

(Received 18 June 2003; accepted 17 July 2003)

We have studied mixtures of alcohol and water in an extensive series of 465 molecular-dynamics simulations with an aggregate length of 713 ns, in order to study excess properties of mixing, in particular the relation between mobility and viscosity. Methanol/water, ethanol/water, and 1-propanol/water mixtures were simulated using an alcohol content of 0–100 mass % in steps of 10%, using the OPLS (optimized potential for liquid simulations) force field for the alcohol molecules and the TIP4P (transferable intermolecular potential with four particles) water model. Computed densities and energies show very good agreement with experimental data for bulk simulations and the mixtures are satisfactory as well. The shear viscosity was computed using nonequilibrium molecular-dynamics simulations. Other properties studied include diffusion constants and rotational correlation times. We find the mobility to correlate well with the viscosity data, i.e., at intermediate alcohol concentrations the viscosity is maximal and the mobility is minimal. Furthermore, we have combined the viscosity and diffusion calculations in order to compute an effective hydrodynamic radius of the particles in the mixtures, using the Stokes–Einstein relation. This analysis indicates that there is no collective diffusion of molecular clusters in these mixtures. For all properties we find that the excess values are underestimated in the simulations, which, given that the pure liquids are described rather well, raises the question whether the potential function is too simplistic to describe mixtures quantitatively. The set of simulations presented here can hence be regarded as a force-field benchmark. [DOI: 10.1063/1.1607918]

I. INTRODUCTION

Water/alcohol mixtures can be regarded as simple model systems for studying the hydrophobic effect. With increasing chain length the solubility of alcohols in water decreases, due to aggregation of aliphatic groups. A recent neutron-diffraction study of a methanol/water mixture[1] has provided direct structural proof for the hypothesis that molecular segregation occurs even for the shortest alcohol in aqueous solution. Indirect evidence for microscopic phase separation can be found from, e.g., dielectric relaxation measurements. Sato *et al.* have shown in a series of publications that the thermodynamics of mixing of short alcohols (methanol,[2] ethanol,[3] 1-propanol,[4] and 2-propanol[5]) with water are complex functions of the liquid composition.

An obvious advantage of studying alcohols over, e.g., alkanes is that they are in fact soluble, allowing direct studies of hydration, and the effect of chain length on properties. Textbook physical chemistry[6] shows that in an ideal mixture the enthalpy of mixing is zero, but mixing is favored due to entropy. For water/alcohol mixtures there is considerable negative excess enthalpy, at least for the shorter alcohols. In fact, for real (nonideal) mixtures most properties show nonideal mixing behavior, for instance in water/alcohol mixtures there is a large excess viscosity upon mixing.[7] Measurement of properties of mixtures is labor intensive and it would be beneficial if properties could be predicted accurately, and preferably at low cost. In order to stimulate computer based predictions, a competition, sponsored by the chemical industry,[8] was held with the objective of predicting fluid properties like density and viscosity of mixtures. Molecular-dynamics simulations[9–11] could be a valuable tool in this respect, as they allow prediction of equilibrium as well as nonequilibrium properties.

A number of studies on alcohol/water mixtures in atomic detail have been published, aimed at studying details of interactions, e.g., density of mixing of methanol and water[12,13] and structural properties.[1,14–20] A systematic analysis of the relation between transport properties at the molecular level (translational and rotational mobility) and the macroscopic level (viscosity) by simulation has hitherto not been done for mixtures of molecules. Van der Spoel has presented an analysis of simulations of 1-octanol aggregation in water[21] where special attention was paid to the relation between water mobility and the hydrophobic effect. However, that analysis yields only qualitative information due to the nonequilibrium nature of the aggregation process. Here we present results from an extensive and systematic series of simulations of

[a)]Fax: 46-18-511755; electronic mail: spoel@xray.bmc.uu.se

TABLE I. Overview of methanol/water simulations, number of molecules, alcohol mass fraction M(%), and mole fraction X. Equilibrium properties of the mixtures. Experimental density from Ref. 31.

H_2O	MeOH	M(%)	X	ρ (g/l) Simul.	ρ (g/l) Expt.	E_{inter} (kJ/mole)
1000	0	0	0.0	994.3±0.2	996.34	−41.37±0.01
900	56	10	0.059	973.1±0.2	979.68	−41.15±0.00
800	112	20	0.123	952.9±0.2	963.52	−40.85±0.00
700	169	30	0.194	932.9±0.4	947.18	−40.46±0.01
600	225	40	0.273	913.1±0.3	929.10	−39.99±0.01
500	281	50	0.360	893.3±0.2	909.76	−39.42±0.01
400	337	60	0.457	872.9±0.3	888.18	−38.73±0.00
300	394	70	0.568	851.3±0.2	864.36	−37.87±0.01
200	450	80	0.692	828.1±0.1	839.74	−36.78±0.00
100	506	90	0.835	802.3±0.5	812.68	−35.30±0.01
0	562	100	1.0	773.0±0.2	783.56	−33.20±0.01

shorter (soluble) alcohols in order to study the effects of mixing on mobility and viscosity. An interesting question that we would like to answer is whether the relation between simultaneous slow diffusion and high viscosity in mixtures can be explained by diffusion of entities larger than single molecules. Before addressing this issue, we have to assess whether simulation methods (and force fields) are accurate enough to model mixtures. The set of simulations presented here could well be regarded as a stringent test of force field quality, since we present both simulation data and reference experimental data in order to facilitate future comparisons of models with experiment.

II. METHODS

A. Equilibrium molecular-dynamics simulations

All simulations used the OPLS (optimized potential for liquid simulations) force field[22,23] for the alcohol molecules and the TIP4P (transferable intermolecular potential with four particles) water model,[24] in part because early simulations of methanol/water systems were shown to reproduce the excess properties of mixing at room temperature rather well.[25] Lennard-Jones parameters for interactions between different atom types were derived from combination rules:

$$\sigma_{ij}=\sqrt{\sigma_i\sigma_j},\quad \epsilon_{ij}=\sqrt{\epsilon_i\epsilon_j}, \tag{1}$$

where σ is the van der Waals radius and ϵ is the depth of the potential well. The particle-mesh Ewald (PME) algorithm[26,27] was used for long-range electrostatics interactions. Although the OPLS force field was parametrized for use with a cutoff, and hence energy and density may be slightly off, we think that long-range ordering may be present even in molecular liquids and mixtures. In the case of pure water it was found that correlations exist at least up to 1.4 nm,[28] and hence long-range interactions cannot be neglected. Similarly, long-range interactions were also found to be important for protein stability.[29] On the other hand, in simulations of fluids the differences due to inclusion of long-range electrostatics were found to be small.[30] In the development of the parameter set for organic molecules, Jorgensen *et al.* used different cutoffs, e.g., for short alcohols 1.1 nm was used but for 1-propanol 1.5 nm.[22] Here we decided to use a 1.1-nm cutoff for Lennard-Jones interactions with analytic long-range corrections to energy and virial[9] whereas the Coulomb interactions are treated by the PME algorithm. A complete overview of the simulation systems is given in Tables I–III.

For all 31 systems a series of five starting configurations was generated using a preliminary series of simulations. With all different coordinates we performed equilibration/production simulations of 2.2 ns (155 in total), under con-

TABLE II. Overview of ethanol/water simulations, number of molecules, alcohol mass fraction M(%), and mole fraction X. Equilibrium properties of the mixtures. Experimental density from Ref. 31.

H_2O	EtOH	M(%)	X	ρ (g/l) Simul.	ρ (g/l) Expt.	E_{inter} (kJ/mole)
1000	0	0	0.0	994.3±0.2	997.08	−41.37±0.01
900	39	10	0.042	977.1±0.1	980.43	−41.54±0.01
800	78	20	0.088	960.7±0.2	966.39	−41.64±0.01
700	117	30	0.143	943.8±0.3	950.67	−41.68±0.01
600	156	40	0.206	925.7±0.3	931.48	−41.65±0.01
500	196	50	0.281	906.1±0.3	909.85	−41.53±0.01
400	235	60	0.370	886.4±0.4	886.99	−41.35±0.01
300	274	70	0.477	865.5±0.3	863.40	−41.10±0.01
200	313	80	0.610	843.8±0.4	839.11	−40.72±0.02
100	352	90	0.779	820.4±0.3	813.62	−40.12±0.02
0	391	100	1.0	792.7±0.4	785.06	−38.94±0.02

TABLE III. Overview of 1-propanol/water simulations, number of molecules, alcohol mass fraction $M(\%)$, and molar fraction X. Equilibrium properties of the mixtures. Experimental density from Ref. 31.

				ρ (g/l)		E_{inter}
H_2O	PrOH	$M(\%)$	X	Simul.	Expt.	(kJ/mole)
1000	0	0	0.0	994.3±0.2	997.97	−41.37±0.01
900	30	10	0.032	978.5±0.2	985.07	−41.58±0.00
800	60	20	0.070	960.6±0.5	969.63	−41.72±0.01
700	90	30	0.113	941.4±0.3	950.30	−41.84±0.00
600	120	40	0.167	921.5±0.2	929.60	−41.95±0.01
500	150	50	0.231	901.6±0.1	908.77	−42.06±0.01
400	180	60	0.310	881.7±0.4	888.37	−42.18±0.01
300	210	70	0.412	862.6±0.2	867.93	−42.35±0.01
200	240	80	0.545	842.9±0.2	847.53	−42.52±0.01
100	270	90	0.730	823.0±0.2	826.70	−42.80±0.02
0	300	100	1.0	799.7±0.4	803.73	−42.94±0.05

stant temperature and pressure using the Berendsen algorithm[32] at a temperature of 25 °C and a pressure of 1 bar. Coupling constants were 0.1 ps for temperature and 1.0 ps for pressure. In all simulations a time step of 2 fs was employed with the leap-frog integrator.[33] The SETTLE algorithm[34] was used to maintain the geometry of the water molecules, whereas the bonds in the alcohol molecules were constrained using the SHAKE algorithm.[35] Neighbor lists were used and updated every 10 fs. Energies and coordinates were stored every 100 fs.

B. Nonequilibrium simulations

A number of methods exist to determine the viscosity from equilibrium simulation, e.g., the Green–Kubo method and the Einstein method.[9] These methods are based on the autocorrelation function (ACF) of the pressure tensor, where the ACF of the off-diagonal elements is related to shear viscosity and the ACF of the diagonal is related to bulk viscosity,

$$\eta = \frac{V}{k_B T} \int_0^\infty \langle P_{\alpha\beta} P_{\alpha\beta} \rangle dt, \tag{2}$$

where V is the volume, T is the temperature, and k_B is Boltzmann's constant. The pressure tensor elements are difficult to obtain accurately, however, because of the large fluctuations in the pressure in MD simulations. As a result, the convergence of these methods is very slow. To improve slightly on this, one can average over the three independent values (P_{xy}, P_{xz}, P_{yz}) for the shear viscosity and (P_{xx}, P_{yy}, P_{zz}) for the bulk viscosity.

Recently, Hess has performed a comparison of methods for determining the shear viscosity from computer simulations.[36] He extensively tests the so-called periodic perturbation (PP) method, originating in the work of Gosling *et al.*,[37] in which a spatially periodic forcing function is imposed on the system, and the shear viscosity can be determined from the response of the system to the applied function (note that a very similar method was described almost simultaneously[38]). The applied periodic forcing function is a sinusoidal:

$$F_{i,x} = m_i \mathcal{A} \cos(kz), \tag{3}$$

where k is the wave-index number, z the z coordinate of the particle i in the simulation box, m_i is the mass of the particle, and A is the applied acceleration. The resulting steady-state velocity profile for macroscopic liquids follows from integrating the Navier–Stokes equations:

$$u_x(z) = \mathcal{V}(1 - e^{-t/\tau_r}) \cos(kz), \tag{4}$$

$$\mathcal{V} = \mathcal{A} \frac{\rho}{\eta k^2}, \tag{5}$$

$$\tau_r = \frac{\rho}{\eta k^2}, \tag{6}$$

where τ_r is the macroscopic relaxation time of the liquid (the time for a certain momentum fluctuation in the liquid to have fully decayed due to viscous dissipation). The viscosity η can be obtained by calculating $\mathcal{V}$ directly from the simulations. Hess[36] mentions a number of criteria to be fulfilled in order to obtain a correct value for the velocity, the most important of which are:

(i) the Navier–Stokes equations are for macroscopic liquids, therefore the reciprocal maximum shear rate should be longer then the rotational correlation time of a molecule (see also Ref. 39);
(ii) the wavelength of the imposed acceleration should be an order of magnitude larger than the size of a molecule (ideally the wave number should go to zero[9]).

Two sets of simulations were performed using the periodic perturbation method. First, a set with the same simulation boxes as were used for the equilibrium simulations. Here the amplitude of the imposed acceleration $\mathcal{A}$ [Eq. (3)] was 0.1 nm/ps^2. Five independent simulations of 1.2 ns each were performed of all systems, using the constant pressure algorithm.[32] For each of these the first 200 ps were dropped and the viscosity was calculated for each simulation and then averaged. In the results this data set will be referred to as PP1. A further set of simulations was performed in which three boxes were stacked in the Z direction, making the system three times as large (requirement ii above). Here, we use an acceleration of 0.01 nm/ps^2 in order to minimize the influence on the dynamics of the molecules. These simulations

TABLE IV. Heat of vaporization ΔH_{vap} of the pure liquids is computed from the equilibrium simulations using Eq. (7) compared to experimental values at 298.15 K. Gas phase energy $E_{\text{intra}}(g)$ of the four molecules in our simulation protocol. All energies are in kJ/mole.

Molecule	ΔH_{vap} Simul.	ΔH_{vap} Expt.	$E_{\text{intra}}(g)$
Water	43.86±0.01	43.99	0
Methanol	35.69±0.01	37.4	23.28
Ethanol	41.43±0.02	42.3	20.30
1-propanol	45.43±0.05	47.5	27.44

were performed at constant volume, at the densities that were obtained from the equilibrium simulations (see Tables I–III). The viscosity data set from these simulations will be referred to as PP2.

In total, 155 equilibrium simulations (of 2.2 ns) and 310 nonequilibrium simulations (of 1.2 ns) were performed using the GROMACS software.[40,41] Due to excellent software optimizations, the entire simulation set took less than 10 000 CPU hours on Intel Xeon processors.

III. RESULTS

Equilibration of the simulations was checked by monitoring the potential energy and density. In all cases these values had equilibrated within 50 ps. To be on the safe side, we used a margin of 200 ps which were left for equilibrating, leaving 2 ns of the equilibrium simulations and 1 ns of the viscosity simulations, respectively, for analysis.

A. Thermodynamics

The enthalpy of vaporization ΔH_{vap} for the liquids can be computed from

$$\Delta H_{\text{vap}} = [E_{\text{intra}}(g) + k_B T] - [E_{\text{intra}}(l) + E_{\text{inter}}(l)]. \quad (7)$$

For water the intramolecular $E_{\text{intra}}(g)$ is zero, for the other molecules it was computed by performing an extra simulation of single molecules of methanol, ethanol, and 1-propanol under the same conditions as the bulk simulations (including the PME algorithm[27]). In Table IV the resulting ΔH_{vap} values are compared to the experimental values. Water and ethanol are very good (within 1 kJ/mole), whereas methanol and 1-propanol both are slightly too low.

The intermolecular energies of the mixtures were computed from the potential energy $E_{\text{pot}} = E_{\text{intra}}(l) + E_{\text{inter}}(l)$ by subtracting the intramolecular energy in gas phase (since we do not know the intramolecular energy in the liquid phase):

$$E_{\text{inter}} = \frac{E_{\text{pot}} - N_W E_{\text{intra},W}(g) - N_A E_{\text{intra},A}(g)}{N_W + N_A}, \quad (8)$$

where N_W and N_A are the number of water and alcohol molecules, respectively. The resulting values are listed in Tables I–III. The excess heat of mixing ΔH_{mix} can be determined from

$$\Delta H_{\text{mix}} = \frac{E_{\text{pot}} - N_W E_{\text{inter},W} - N_A E_{\text{inter},A}}{N_W + N_A}, \quad (9)$$

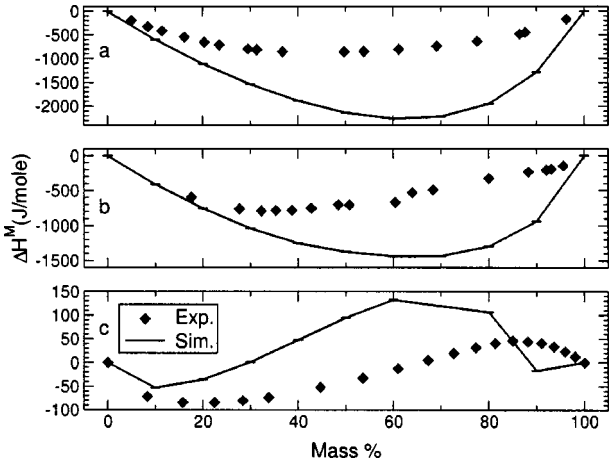

FIG. 1. Excess heat of mixing as a function of the mass percentage for **a**: methanol/water (experimental data from Ref. 42), **b**: ethanol/water (experimental data from Ref. 43), and **c**: 1-propanol/water (experimental data from Ref. 44).

where $E_{\text{inter},W}$ and $E_{\text{inter},A}$ are determined from Eq. (8) for the pure substances. Simulated and experimental ΔH_{mix} are plotted in Fig. 1.

The simulation results are qualitatively correct, although the excess energies are overestimated, probably due to the enhanced dipole moment of both the TIP4P water model and the alcohols, which may be inappropriate in a mixture with alcohols. Even the shape of the ΔH_{mix} curve for 1-propanol/water, with negative values for low alcohol concentrations, and positive values for high concentration is reproduced qualitatively. Over all, the energies are reproduced within 2 kJ/mole over the whole composition range, in all mixtures.

The simulated densities are tabulated in Tables I–III alongside experimental densities. The values for the pure compounds are in excellent agreement with the experimental values, methanol has a density that is 1.4% too low, for the other molecules the difference is less than one percent. Excess densities are plotted in Fig. 2. We see that excess properties are qualitatively correct, however, their maxima are too low compared to experiments by 8 g/l (methanol), 6 g/l

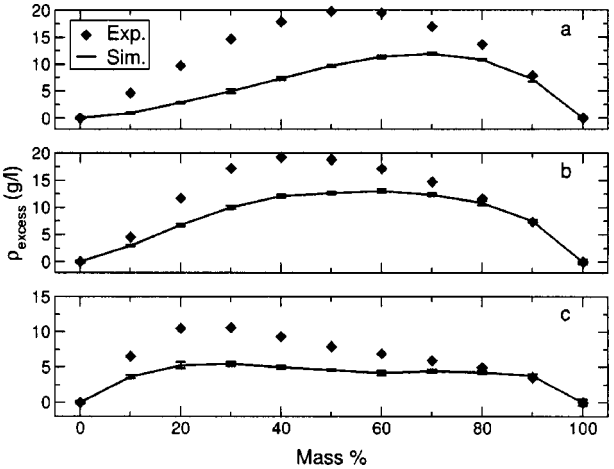

FIG. 2. Simulated and experimental excess density as a function of the mass percentage for **a**: methanol, **b**: ethanol, and **c**: 1-propanol/water mixtures.

TABLE V. Values for the self-diffusion coefficient D (10^{-9} m^2/s) of the alcohols in mixtures, computed from five simulations of 2 ns. The first column gives the mass percentage of the alcohols in water. The given errors are the statistical best estimates of the error in a calculated mean. Experimental values were determined from a cubic spline interpolation/extrapolation of the data from Ref. 45 (MeOH/water), Refs. 46 and 47 (EtOH/water), and Ref. 48 (PrOH/water), respectively.

	MeOH/water		EtOH/water		1-PrOH/water	
%	Simul.	Expt.	Simul.	Expt.	Simul.	Expt.
0		1.57		1.24		1.00
10	2.28±0.3	1.32	1.76±0.3	0.93	1.42±0.2	0.60
20	2.10±0.3	1.16	1.36±0.15	0.74	1.03±0.11	0.35
30	1.99±0.11	1.09	1.15±0.11	0.64	1.02±0.14	0.15
40	1.87±0.15	1.07	1.10±0.10	0.61	0.90±0.09	0.12
50	1.80±0.16	1.10	1.03±0.10	0.62	0.83±0.07	0.14
60	1.81±0.09	1.18	1.00±0.08	0.65	0.76±0.05	0.19
70	1.91±0.09	1.31	0.92±0.08	0.70	0.72±0.04	0.25
80	2.12±0.08	1.51	1.02±0.06	0.78	0.73±0.03	0.33
90	2.41±0.14	1.83	1.08±0.11	0.89	0.74±0.03	0.47
100	3.19±0.06	2.37	1.40±0.06	1.08	0.85±0.04	0.74

(ethanol), and 5 g/l (1-propanol), respectively. Although these absolute errors are comparable in magnitude to the errors in the densities of pure substances, the densities of the pure substances have been subtracted out. Therefore we have computed the relative error in the density defined as $1-\rho_{\mathrm{sim}}/\rho_{\mathrm{exp}}$ (data not shown). In all cases the relative error is below 1.5% of the density, and the effect of mixing on the relative error is minor.

B. Mobility

The translational mobility of molecules is best described by the diffusion constant. Self-diffusion describes the process of motion in a medium consisting of similar molecules. For water the self-diffusion constant D is 2.3×10^{-5} cm^2/s,[49,50] a value that is difficult to reproduce in simulations using simple classical models.[51] The TIP4P model we have used in this work has a diffusion constant which is too high (like most models). Diffusion in mixtures can be determined as self diffusion,[45,48,52–54] or as mutual diffusion.[55–57] Mutual diffusion is a collective property that determines how fast two (or more) components mix, whereas self-diffusion describes the translational mobility of individual molecules in the mixture. The relation between self-diffusion and mutual diffusion is not straightforward[58] and has hitherto only been studied by simulation for simple Lennard-Jones particles.[59] Here we are mainly interested in the relation between molecular mobility and viscosity. Self-diffusion constants for water and alcohol were computed from the mean-square displacement (MSD) using the Einstein relation,[9] by splitting each of the five 2-ns trajectories in four bits of 500 ps, and averaging the MSD. The resulting values for all simulations are given in Table V, Table VI, and Fig. 3. Both water and methanol show a minimum in the diffusion as a function of mass percentage in the methanol/water mixtures. For water in the other mixtures the diffusion decreases with mass percentage. Water in ethanol/water mixtures experimentally[54] has a slight maximum at 70% which is not reproduced in the simulation (see Table VI).

We have also studied relaxation processes of the water and alcohol molecules, which can in principle be determined experimentally by NMR. The relaxation properties can be characterized by reorientational correlation functions:

$$C_l^{\alpha}=\langle P_l[\mathbf{e}^{\alpha}(t)\cdot\mathbf{e}^{\alpha}(0)]\rangle, \tag{10}$$

where P_l is the lth rank Legendre polynomial and $\mathbf{e}^{\alpha}$ is the unit vector which points along the α axis in the molecular reference frame. For our analyses we have used only one axis, the one parallel to the molecular dipole μ which is related to dielectric relaxation of the bulk liquid. We have computed both the first and second rank Legendre polynomials. Our previous analysis of the rotational correlation of different water models[51] showed that there is an almost constant factor between first and second rank Legendre polynomial descriptions of the rotational motion. We find (Table

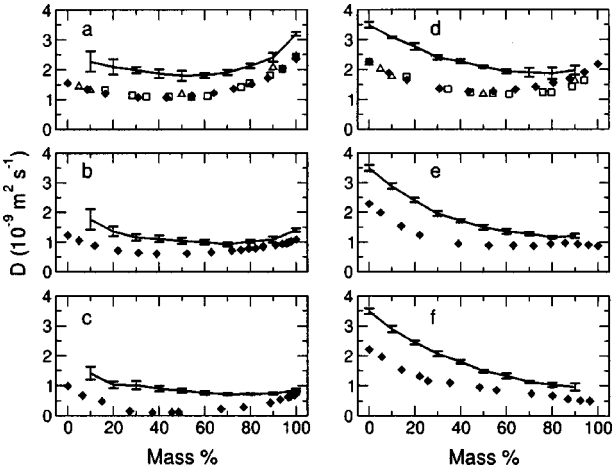

FIG. 3. Diffusion constants in the mixtures as determined from the Einstein relation of the mean-square displacement. **a**: diffusion of methanol [experimental values ♦ (Ref. 45), □ (Ref. 52), △ (Ref. 53)], **b**: ethanol (experimental values from Refs. 46 and 47), **c**: 1-propanol (experimental values from Refs. 48 and 55), **d**: water in methanol/water [experimental values ♦ (Ref. 45), □ (Ref. 52), △ (Ref. 53)], **e**: water in ethanol/water [experimental value ♦ (Ref. 54)], **f**: water in 1-propanol/water (experimental values from Ref. 48).

TABLE VI. Values for the self-diffusion coefficient D (10^{-9} m^2/s) of water in the mixtures, computed from five simulations of 2 ns. The first column gives the mass percentage of the alcohols in water. The given errors the statistical best estimates of the error in a calculated mean. Experimental values were determined from a cubic spline interpolation/extrapolation of the data from Ref. 45 (MeOH/water), Ref. 54 (EtOH/water), and Ref. 48 (PrOH/water), respectively.

	MeOH/water		EtOH/water		1-PrOH/water	
%	Simul.	Expt.	Simul.	Expt.	Simul.	Expt.
0	3.50±0.10	2.28	3.50±0.10	2.3	3.50±0.10	2.22
10	3.08±0.03	1.84	2.89±0.10	1.72	2.90±0.11	1.74
20	2.78±0.11	1.57	2.41±0.07	1.30	2.45±0.07	1.38
30	2.40±0.07	1.39	1.96±0.08	1.06	2.07±0.08	1.14
40	2.28±0.07	1.28	1.72±0.06	0.94	1.81±0.06	1.05
50	2.09±0.04	1.26	1.50±0.08	0.89	1.49±0.05	0.93
60	1.94±0.07	1.31	1.35±0.09	0.90	1.34±0.09	0.83
70	1.90±0.15	1.39	1.28±0.06	0.88	1.13±0.04	0.76
80	1.87±0.20	1.56	1.16±0.05	0.94	1.04±0.08	0.68
90	1.98±0.15	1.77	1.21±0.07	0.93	0.96±0.12	0.54
100		2.19		0.87		0.49

VII) that the ratio is roughly three here too. Furthermore, the results obtained for TIP4P water with the PME algorithm ($\tau_1=2.9$ ps, $\tau_2=1.0$ ps) are comparable with the results we obtained before with a cutoff ($\tau_1=3.4$ ps, $\tau_2=1.1$ ps) or reaction field ($\tau_1=2.7$ ps, $\tau_2=1.0$ ps).[51] In the rotation correlation times of the alcohols we note that methanol has a maximum at 70 mass %, and ethanol has a maximum at 90 mass %, while 1-propanol does not have a maximum. For water in all mixtures the correlation times increase monotonously.

C. Viscosity

The viscosity was calculated using the periodic perturbation (PP) method in two sets of simulations, named PP1 and PP2 (see the Methods section). The criteria for obtaining the correct viscosity from a simulation (see Methods) were checked for the PP1 set by comparing the rotational correlation times (τ_1 *in the nonequilibrium simulations, i.e., not those from Table VII*) to the momentum fluctuation relaxation time τ_r [Eq. (6)]. It was found that the $\tau_1<\tau_r$ in all cases, although not by a large margin. This automatically implies that $\tau_1<\tau_r$ in the PP2 set, where the external acceleration was only one-tenth of the one in the PP1 set.

The simulated viscosities are shown in Tables VIII–X along with the experimental values. The PP2 data set is consistently better than PP1 when compared to experiment, yet the viscosities are still rather low. A reason why the PP method yields values that are too low could be that the acceleration exerted was too large. Alcohol rotation correlation times in the nonequilibrium simulations (PP1) were systematically shorter (by 0.5–2 ps) than in the equilibrium simulations (data not shown). For the PP2 set the differences were negligible. It is unclear therefore whether the magnitude of the imposed acceleration can explain the whole deviation from experiment. In principle our results could be hampered by finite wavelength,[9] however, since we have used two different sizes of the computational cell, the larger one with a much reduced acceleration A [Eq. (3)] this seems unlikely too. The excess viscosities, in excess of linearity with alcohol fraction, are plotted in Fig. 4. The excess viscosity for both PP sets are smooth functions of the alcohol concentration but well below the experimental values for all of the

TABLE VII. Rotational correlation times, for **a**: alcohol, and **b**: water molecules obtained by integration of the dipole correlation function after fitting its tail with an exponential function. First- and second-order Legendre polynomials were used, yielding two rotational correlation times: τ_1 and τ_2. Values were computed from the average correlation function of five simulations of 2.2 ns each.

	MeOH/water				EtOH/water				PrOH/water			
	MeOH		Water		EtOH		Water		PrOH		Water	
%	τ_1	τ_2	τ_1	τ_2	τ_1	τ_2	τ_1	τ_2	τ_1	τ_2	τ_1	τ_2
			2.9	1.0			2.9	1.0			2.9	1.0
10	3.8	1.3	3.4	1.2	5.9	2.0	3.7	1.3	7.6	2.4	3.6	1.3
20	4.5	1.4	4.1	1.4	7.2	2.3	4.5	1.6	8.8	2.7	4.3	1.5
30	5.1	1.6	4.8	1.6	8.4	2.7	5.5	1.9	10.1	3.0	4.9	1.7
40	5.7	1.8	5.5	1.9	9.6	3.0	6.4	2.2	11.3	3.3	5.6	1.9
50	6.4	1.9	6.3	2.1	10.8	3.2	7.5	2.5	12.4	3.6	6.4	2.2
60	6.9	2.0	7.1	2.3	12.0	3.5	8.7	2.8	13.3	3.8	7.4	2.5
70	7.2	2.1	8.0	2.5	12.9	3.7	10.0	3.2	15.0	4.2	8.8	2.8
80	7.1	2.1	8.6	2.7	13.8	3.9	11.7	3.6	16.3	4.6	10.6	3.3
90	6.6	1.9	8.8	2.7	14.2	3.9	13.5	4.0	18.3	5.0	13.8	4.0
100	5.3	1.6			12.7	3.5			18.8	5.3		

TABLE VIII. Methanol/water viscosity $\eta\,(10^{-3}$ P) with standard deviation as a function of liquid composition computed using the periodic perturbation method. Experimental data from Ref. 60.

%	Simul. (PP1)	Simul. (PP2)	Expt.
0	4.64±0.03	4.79±0.09	8.95
10	5.40±0.03	5.82±0.14	11.58
20	6.21±0.04	6.59±0.12	14.00
30	6.63±0.05	7.26±0.15	15.31
40	7.10±0.05	7.87±0.16	15.93
50	7.31±0.06	7.90±0.17	15.10
60	7.18±0.06	7.80±0.16	14.03
70	6.72±0.05	7.31±0.08	11.90
80	5.81±0.04	6.57±0.12	10.06
90	4.68±0.05	5.44±0.14	7.67
100	3.27±0.03	3.97±0.06	5.41

TABLE X. 1-propanol/water viscosity $\eta\,(10^{-3}$ P) with standard deviation as a function of liquid composition computed using the periodic perturbation method. Experimental data from Ref. 61.

%	Simul. (PP1)	Simul. (PP2)	Expt.
0	4.64±0.03	4.79±0.09	8.95
10	6.09±0.04	6.51±0.07	13.47
20	7.62±0.05	8.48±0.25	18.36
30	8.95±0.08	9.72±0.27	22.26
40	10.11±0.10	11.66±0.42	24.97
50	11.11±0.12	13.05±0.48	26.50
60	11.97±0.15	14.12±0.26	26.61
70	11.82±0.14	14.64±0.51	25.92
80	11.35±0.13	14.83±0.75	23.94
90	10.72±0.13	14.36±0.47	21.62
100	8.15±0.09	11.89±0.41	19.38

three different alcohol mixtures. The PP2 is slightly better than PP1 for ethanol/water, but otherwise the differences are negligible. It seems therefore that the magnitude of the excess viscosity is determined by the force field rather than the exact simulation conditions. The maximum in the excess viscosities have shifted somewhat to the higher alcohol concentrations, where in the experiments is found to be at the lower alcohol concentrations.

D. Correlation between the diffusion coefficient and the viscosity

In order to study the correlation between diffusion and viscosity we define an average diffusion constant D_m as

$$D_m=(1-x)D_w+xD_a\,, \tag{11}$$

where D_w and D_a are the self-diffusion coefficients of water and alcohol, respectively (Tables V and VI), and x is the mole fraction of alcohol. Likewise, we have computed the average rotational correlation time τ_{1m} from

$$\tau_{1m}=(1-x)\tau_{1w}+x\tau_{1a}\,, \tag{12}$$

where τ_{1w} and τ_{1a} are the τ_1 rotational correlation times of water and alcohol, respectively (Table VII). The correlations between D_m, τ_{1m}, and the viscosity η (PP2 data set) in our simulations are plotted in Fig. 5. Although there is a clear correlation between inverse diffusion coefficient and viscosity, the relation is strongly composition dependent: a given value of D_m (or τ_{1m} for that matter) can correspond to different viscosities. Furthermore, there is an obvious correlation between rotational correlation and the inverse diffusion coefficient, but here too, we find that the curves are composition dependent.

The Stokes–Einstein relation relates diffusion to viscosity:

$$D=\frac{k_BT}{6\pi\eta r}, \tag{13}$$

where k_B is Boltzmann's constant, T is the temperature, and r is the hydrodynamic radius of the particle. We have computed the effective hydrodynamic radius in our mixture simulations using D_m [Eq. (11)]. In order to compare the results to experiments we interpolated the experimental self-diffusion coefficients (Tables V and VI). The resulting radii are plotted in Fig. 6, using viscosities from both the PP1 and PP2 data sets. We see an obvious trend upwards as the alcohol concentration increases. The simulated values are higher than the experimental, mainly because the viscosity is underestimated. Although diffusion is faster in the simulations

TABLE IX. Ethanol/water viscosity $\eta\,(10^{-3}$ P) with standard deviation as a function of liquid composition computed using the periodic perturbation method. Experimental data from Ref. 7.

%	Simul. (PP1)	Simul. (PP2)	Expt.
0	4.64±0.03	4.79±0.09	8.94
10	6.05±0.04	6.33±0.24	13.23
20	7.51±0.06	8.05±0.15	18.15
30	8.83±0.08	9.56±0.36	21.8
40	10.14±0.10	10.85±0.28	23.5
50	10.91±0.11	12.21±0.23	24.0
60	11.17±0.12	12.71±0.28	22.4
70	11.13±0.13	12.92±0.41	20.37
80	9.95±0.11	11.56±0.53	17.48
90	8.39±0.09	10.47±0.30	14.24
100	7.26±0.12	7.98±0.16	10.96

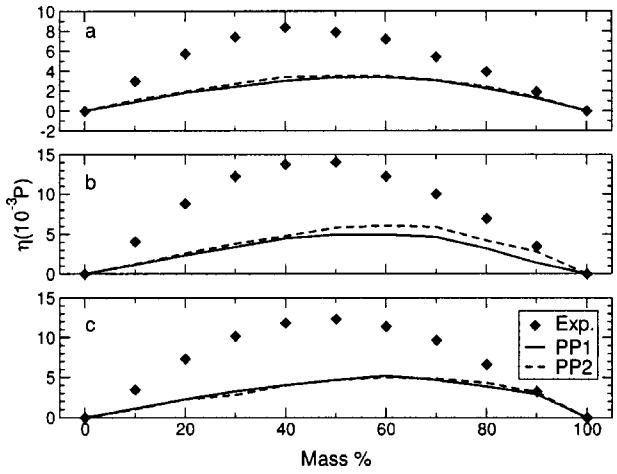

FIG. 4. Excess viscosity as a function of the mass percentage for **a**: methanol, **b**: ethanol, and **c**: 1-propanol/water mixtures. For clarity the error bars (Tables VIII–X) were omitted. Experimental data from Refs. 7, 60 and 61.

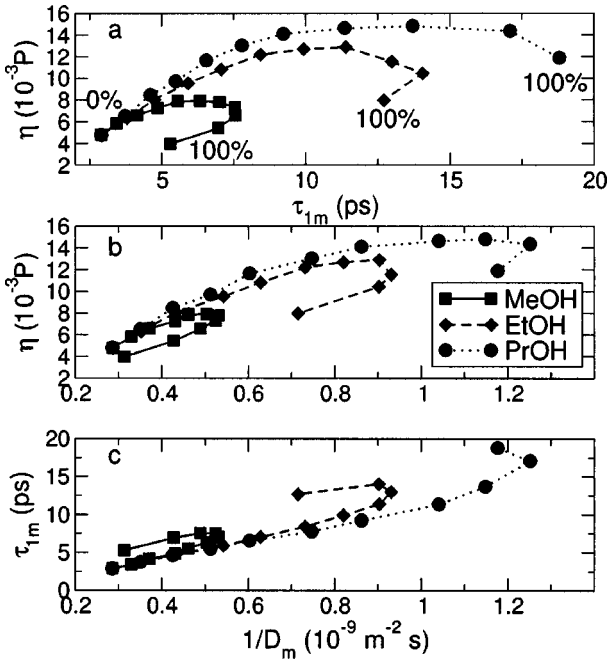

FIG. 5. **a**: correlation between viscosity η and average rotational correlation time τ_{1m} [Eq. (12)], **b**: correlation between viscosity η and inverse average diffusion constant $1/D_m$ [Eq. (11)], **c**: correlation between and average rotational correlation time τ_{1m} and inverse average diffusion constant $1/D_m$. Viscosity was computed using the PP method.

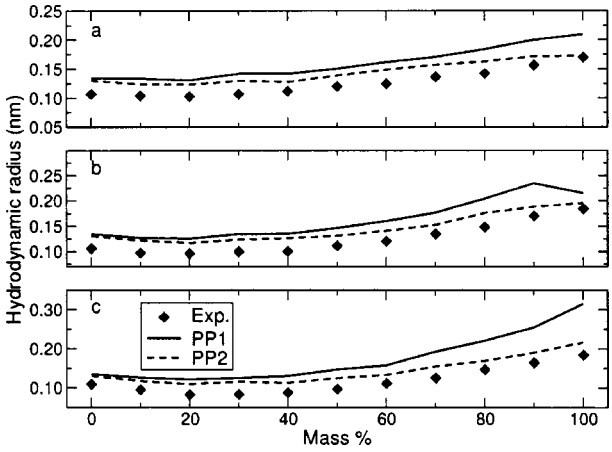

FIG. 6. Effective hydrodynamic radius as function of alcohol mass percentage, computed according to Eq. (13). **a**: methanol/water mixture, **b**: ethanol/water, **c**: 1-propanol/water. Hydrodynamic radii computed using different viscosities (PP1 and PP2) are shown.

than in experiment, this does not compensate completely for the lower viscosity, nevertheless the PP2 set does approach the experimental radii quite well.

IV. DISCUSSION

Quantitative prediction of physical properties from computer simulation is (and should be) the aim of molecular modeling. A lot of progress has been made over the years, some of the authors have, for instance, recently demonstrated the accurate reproduction of ligand binding sites to enzymes by molecular docking.[62] In the realm of industrial applications of molecular modeling, properties of fluids and fluid mixtures are of paramount importance within process technology. The amount of optimism among researchers about the applicability of simulations in the field varies from low[63] to considerable.[64] One of our long-standing interests is to describe interactions between fine, solid particles in the presence of liquids and liquid mixtures.[65] It is with this in mind, that we are particularly keen on reproducing and predicting properties like diffusivity and viscosity.[66] Lundgren *et al.* have recently done a simulation study of water/ethanol mixtures on a nonpolar (graphite) surface[67] and, interestingly, found microscopic phase separation upon addition of ethanol to water, caused by the presence of the surface. Before applying models to such complicated systems however, it is important to verify that the models are good enough for the purpose. Here we have presented extensive simulations in order to compute mixing properties of the short alcohols and water. Most of the simulated properties are in qualitative agreement with experiments. In particular the thermodynamic variables enthalpy of mixing (Fig. 1) and density (Fig. 2) are well reproduced. Although we find that the absolute errors in the density are less than 1.5% in all cases, we must face the fact that this is roughly the magnitude of the excess effects in liquid mixtures. Nevertheless, the excess properties are reproduced qualitatively, even the complicated enthalpy of mixing of 1-propanol/water mixtures (Fig. 1).

When comparing the excess enthalpy of mixing (Fig. 1) to the excess density (Fig. 2) we note that the density is underestimated, seemingly implying that the interaction between alcohol and water is not strong enough, but simultaneously the excess enthalpy is overestimated, seemingly implying that the interaction is too strong. The combination of these two effects can be attributed to deficiencies in the interaction potential. First, the models include an effective polarization, which may be too strong when different molecules are mixed, and reducing the effective polarization would lead to higher energies and therefore less excess enthalpy of mixing. Second, the repulsion part of the potential (modeled by a $1/r^{12}$) may be too steep to allow the density to increase upon mixing. It may be possible that better results could be obtained with a slightly shallower potential surface like a Buckingham (e^{-r}) or $1/r^{10}$ repulsion. A further possibility would be the introduction of smeared charges instead of point charges.[68] However, both these solutions would require parametrizing force fields. By explicitly adding many body potentials one could overcome the limitation of pair potentials.[69] Polarizable models in principle have the advantage of being phase transferable, however, these too require reparametrization of force fields. A large number of polarizable water models have been proposed (e.g., Refs. 70–75, for reviews, see Refs. 69, 76, and 77), as well as some parameter sets for polarizable liquid alcohols.[78–81] These may serve as starting points for those seeking to improve models (including ourselves[51,73,82]). We think that the simulation series we have presented here can serve as a benchmark for new models. If successful, such improved models could be applied to unravel the anomalous temperature dependence of the hydrophobic effect at the microscopic level.[83–85]

Diffusion coefficient have been studied often by simulation for water models (e.g., Refs. 51 and 86), but also for methanol and methanol/water mixtures.[53,87,88] Hawlicka reported excellent results for self-diffusion using flexible models for water and methanol.[53] Since we use somewhat simpler models with a general purpose force field, it can be justified that our results are not as good. However, it should be realized that the transferability of the OPLS parameters[22,23] is very important for those seeking to study more complex molecules such as proteins. Our results are qualitatively correct, and show the correct trends with increasing molecule size (Fig. 3).

The viscosity of TIP4P water model was estimated to be 4.5×10^{-3} P,[89] respectively 5×10^{-3} P,[90] computed using the Green–Kubo relation [Eq. (2)]. These numbers are in good agreement with the value we get from the PP method (4.6, respectively 4.8). However, for the PP1 set we find that the acceleration we applied was too large, leading to molecules that are too slippery. This may be the effect Walser *et al*. have found in their test of the Stokes–Einstein relation at the molecular level.[91] For the PP2 set it seems that the hydrodamic radii have converged towards the experimental ones (Fig. 6) and hence the viscosity is consistent with the diffusion. Other model properties that might influence the viscosity in simulations, such as the effect of the intramolecular flexibility, were found to be negligible for a number of pure substances, among which is methanol.[92] Further reports of simulated viscosities include methanol/water mixtures, studied using a different nonequilibrium simulation method[93] and a mixture of 2-propanol and water.[94] In both papers the excess viscosity was underestimated (as in this work) whereas the pure components were reproduced rather well.

The relation between viscosity and diffusion has hitherto been studied mainly for Lennard-Jones-type particles.[59,95,96] Here we have extended this work to molecules, and an analysis of the effective hydrodynamic radius of mixtures using the Stokes–Einstein relation [Eq. (13)]. The validity of the Stokes–Einstein relation at the microscopic level was recently challenged by Walser *et al.*[91] The authors find a slight deviation from the Stokes–Einstein relation, but within the error bars of the calculation. This, in combination with other theoretical studies of Lennard-Jones particles,[95] seems to indicate that the Stokes–Einstein relation holds even at the molecular level. This allows us to use the relation to compute the effective hydrodynamic radius of the particles in the mixtures. We have done so (Fig. 6) based on both experimental data and simulation data. All the experimental radii have a minimum at low alcohol concentration, which is somewhat puzzling since it seems to indicate that at this composition the diffusing entities are smaller than a single water molecule, while simultaneously the diffusion is slower and viscosity higher. Nevertheless, the trend is reproduced by the simulations, and if anything, we can conclude that there is no evidence for ''collective diffusion'' in either of the three mixtures at any alcohol concentration. An alternative explanation could be that in pure water the diffusing entities are larger than a single molecule, which seems to be supported by the hypothesis that there are two distinct types of motion in water, with different time constants.[97] This is, however, contradicted by recent spectroscopic experiments.[98]

Finally, we have to ask ourselves whether the OPLS (Refs. 22 and 23) models are good enough to study interactions between fine, solid particles in the presence of different liquids. In our earlier work pure (simple point charge[99]) water was applied to two quartz plates and the forces between them were computed.[65] At small distances between the two opposed surfaces the liquid forms a bridge resulting in a significant increase of the forces between the two surfaces. The magnitude of this effect strongly depends on the properties of the liquid. Since we are initially aiming for qualitative insight, we conclude that application of the OPLS models for water and short alcohols will give us qualitatively correct answers for properties like energy, density, and viscosity.

ACKNOWLEDGMENTS

We would like to thank the Norwegian Research Council (NFR) for financially supporting this research. The national supercomputer center in Linköping, Sweden, the Norwegian consortium for high performance computing (NOTUR) and the Bergen computational physics lab (BCPL), Norway, are acknowledged for allocation of computer time.

[1] S. Dixit, J. Crain, W. C. K. Poon, J. L. Finney, and A. K. Soper, Nature (London) **416**, 829 (2002).
[2] T. Sato, A. Chiba, and R. Nozaki, J. Chem. Phys. **112**, 2924 (2000).
[3] T. Sato, A. Chiba, and R. Nozaki, J. Chem. Phys. **110**, 2508 (1999).
[4] T. Sato, A. Chiba, and R. Nozaki, J. Chem. Phys. **113**, 9748 (2000).
[5] T. Sato and R. Buchner, J. Chem. Phys. **118**, 4606 (2003).
[6] P. W. Atkins, *Physical Chemistry*, fourth edition (Oxford University Press, Oxford, UK, 1990).
[7] R. C. Weast, *Handbook of Chemistry and Physics* (Chemical Rubber Corporation, Cleveland, OH, 1977).
[8] The fluid properties challenge is organized by the National Institute of Standards. Web address: http://www.cstl.nist.gov/FluidSimulationChallenge
[9] M. P. Allen and D. J. Tildesley, *Computer Simulations of Liquids* (Oxford Science, Oxford, 1987).
[10] W. F. van Gunsteren and H. J. C. Berendsen, Angew. Chem., Int. Ed. Engl. **29**, 992 (1990).
[11] D. Frenkel and B. Smit, *Understanding Molecular Simulation: From Algorithms to Applications* (Academic, San Diego, 1996).
[12] P. F. W. Stouten and J. Kroon, Mol. Simul. **5**, 175 (1990).
[13] J. M. Stubbs, B. Chen, J. J. Potoff, and J. J. Siepmann, Fluid Phase Equilib. **183**, 301 (2001).
[14] S. Okazaki, K. Nakanishi, and H. Touhara, J. Chem. Phys. **78**, 454 (1983).
[15] S. Okazaki, H. Touhara, and K. Nakanishi, J. Chem. Phys. **81**, 890 (1984).
[16] A. K. Soper and J. L. Finney, Phys. Rev. Lett. **71**, 4346 (1993).
[17] C. A. Koh, H. Tanaka, J. M. Walsh, K. E. Gubbins, and J. A. Zollweg, Fluid Phase Equilib. **83**, 51 (1993).
[18] L. C. G. Freitas, J. Mol. Struct.: THEOCHEM **101**, 151 (1993).
[19] A. Laaksonen, P. G. Kusalik, and I. M. Svishchev, J. Phys. Chem. A **101**, 5910 (1997).
[20] P. G. Kusalik, A. P. Lyubartsev, D. L. Bergman, and A. Laaksonen, J. Phys. Chem. B **104**, 9533 (2000).
[21] D. van der Spoel (unpublished).
[22] W. L. Jorgensen, D. S. Maxwell, and J. Tirado-Rives, J. Am. Chem. Soc. **118**, 11225 (1996).
[23] W. L. Jorgensen, *Encyclopedia of Computational Chemistry* (Wiley, New York, 1998), Vol. 3, Chap. OPLS Force Fields, pp. 1986–1989.
[24] W. L. Jorgensen, J. Chandrasekhar, J. D. Madura, R. W. Impey, and M. L. Klein, J. Chem. Phys. **79**, 926 (1983).
[25] H. Tanaka and K. E. Gubbins, J. Chem. Phys. **97**, 2626 (1992).
[26] T. Darden, D. York, and L. Pedersen, J. Chem. Phys. **98**, 10089 (1993).

[27] U. Essman, L. Perera, M. L. Berkowitz, T. Darden, H. Lee, and L. G. Pedersen, J. Chem. Phys. **103**, 8577 (1995).
[28] C. Chipot, C. Milot, B. Maigret, and P. A. Kollman, J. Chem. Phys. **101**, 7953 (1994).
[29] J. Åqvist, FEBS Lett. **457**, 414 (1999).
[30] M. Kettler, I. Nezbeda, A. A. Chialvo, and P. T. Cummings, J. Phys. Chem. B **106**, 7537 (2002).
[31] *International Critical Tables of Numerical Data, Physics, Chemistry and Technology*, edited by E. W. Washbrun (Knovel, New York, 2003).
[32] H. J. C. Berendsen, J. P. M. Postma, A. DiNola, and J. R. Haak, J. Chem. Phys. **81**, 3684 (1984).
[33] H. J. C. Berendsen and W. F. van Gunsteren, in *Molecular-Dynamics Simulation of Statistical-Mechanical Systems*, edited by G. Ciccotti and W. G. Hoover (North-Holland, Amsterdam, 1986), pp. 43–65.
[34] S. Miyamoto and P. A. Kollman, J. Comput. Chem. **13**, 952 (1992).
[35] J. P. Ryckaert, G. Ciccotti, and H. J. C. Berendsen, J. Comput. Phys. **23**, 327 (1977).
[36] B. Hess, J. Chem. Phys. **116**, 209 (2002).
[37] E. M. Gosling, I. R. McDonald, and K. Singer, Mol. Phys. **26**, 1475 (1973).
[38] B. L. Holian, J. Chem. Phys. **117**, 9567 (2002).
[39] D. J. Searles and D. J. Evans, J. Chem. Phys. **112**, 9727 (2000).
[40] H. J. C. Berendsen, D. van der Spoel, and R. van Drunen, Comput. Phys. Commun. **91**, 43 (1995).
[41] E. Lindahl, B. A. Hess, and D. van der Spoel, J. Mol. Model. **7**, 306 (2001).
[42] R. F. Lama and B. C.-Y. Lu, J. Chem. Eng. Data **10**, 216 (1965).
[43] J. A. Boyne and A. G. Williamson, J. Chem. Eng. Data **12**, 318 (1967).
[44] E. Bose, Z. Phys. Chem., Stoechiom. Verwandtschaftsl. **LVIII**, 585 (1907).
[45] Z. J. Derlacki, A. J. Easteal, A. V. J. Edge, L. A. Woolf, and Z. Roksandic, J. Phys. Chem. **89**, 5318 (1985).
[46] A. J. Easteal and L. A. Woolf, J. Phys. Chem. **89**, 1066 (1985).
[47] K. R. Harris, P. J. Newitt, and Z. J. Derlacki, J. Chem. Soc., Faraday Trans. **94**, 1963 (1998).
[48] E. Hawlicka and R. Grabowski, J. Phys. Chem. **96**, 1554 (1992).
[49] K. Krynicki, C. D. Green, and D. W. Sawyer, Discuss. Faraday Soc. **66**, 199 (1978).
[50] W. S. Price, H. Ide, and Y. Arata, J. Phys. Chem. A **103**, 448 (1999).
[51] D. van der Spoel, P. J. van Maaren, and H. J. C. Berendsen, J. Chem. Phys. **108**, 10220 (1998).
[52] E. Hawlicka, Ber. Bunsenges. Phys. Chem. **87**, 425 (1983).
[53] E. Hawlicka and D. Swiatla-Wojcik, Phys. Chem. Chem. Phys. **2**, 3175 (2000).
[54] W. S. Price, H. Ide, and Y. Arata, J. Phys. Chem. A **107**, 4784 (2003).
[55] K. R. Harris, T. Goscinska, and H. N. Lam, J. Chem. Soc., Faraday Trans. **89**, 1969 (1993).
[56] K. C. Pratt and W. A. Wakeman, Proc. R. Soc. London, Ser. A **336**, 393 (1974).
[57] K. C. Pratt and W. A. Wakeman, Proc. R. Soc. London, Ser. A **342**, 401 (1975).
[58] Y. Zhou and G. H. Miller, J. Phys. Chem. **100**, 5516 (1996).
[59] Y. Zhou and G. H. Miller, Phys. Rev. E **53**, 1587 (1996).
[60] S. Zhang, H. Li, S. Dai, T. Wang, and S. Han, J. Chem. Eng. Data **42**, 651 (1997).
[61] S. Z. Mikhail and W. R. Kimel, J. Chem. Eng. Data **8**, 323 (1963).
[62] C. Hetényi and D. van der Spoel, Protein Sci. **11**, 1729 (2002).
[63] B. Smit, Fluid Phase Equilib. **116**, 249 (1996).
[64] P. T. Cummings, Fluid Phase Equilib. **116**, 237 (1996).
[65] E. J. W. Wensink, A. C. Hoffmann, M. E. F. Apol, and H. J. C. Berendsen, Langmuir **16**, 7392 (2000).
[66] G. Nägele, J. Phys.: Condens. Matter **15**, S407 (2003).
[67] M. L. Lundgren, N. L. Allan, and T. Cosgrove, Langmuir **18**, 10462 (2002).
[68] B. J. Guillot and Y. Guissani, J. Chem. Phys. **114**, 6720 (2001).
[69] S. W. Rick and S. J. Stuart, Rev. Comput. Chem. **18**, 89 (2002).
[70] P. Ahlström, A. Wallqvist, S. Engström, and B. Jönsson, Mol. Phys. **68**, 563 (1989).
[71] L. X. Dang and T. M. Chang, J. Chem. Phys. **106**, 8149 (1997).
[72] B. Chen, J. Xing, and J. I. Siepmann, J. Phys. Chem. B **104**, 2391 (2000).
[73] P. J. van Maaren and D. van der Spoel, J. Phys. Chem. B **105**, 2618 (2001).
[74] H. Saint-Martin, J. Hernández-Cobos, M. I. Bernal-Uruchurtu, I. Ortega-Blake, and H. J. C. Berendsen, J. Chem. Phys. **113**, 10899 (2000).
[75] P. Ren and J. W. Ponder, J. Phys. Chem. B **107**, 5933 (2003).
[76] S.-B. Zhu, S. Singh, and G. W. Robinson, Adv. Chem. Phys. **85**, 627 (1994).
[77] B. Guillot, J. Mol. Liq. **101**, 219 (2002).
[78] J. L. Gao, D. Habibollazadeh, and L. Shao, J. Phys. Chem. **99**, 16460 (1995).
[79] J. Hernandez-Cobos and I. Ortega-Blake, J. Chem. Phys. **103**, 9261 (1995).
[80] J. W. Caldwell and P. A. Kollman, J. Phys. Chem. **99**, 6208 (1995).
[81] M. A. Gonzalez, E. Enciso, F. J. Bermejo, and M. Bee, J. Chem. Phys. **110**, 8045 (1999).
[82] P. C. Jordan, P. J. van Maaren, J. Mavri, D. van der Spoel, and H. J. C. Berendsen, J. Chem. Phys. **103**, 2272 (1995).
[83] K. A. T. Silverstein, A. D. J. Haymet, and K. A. Dill, J. Chem. Phys. **111**, 8000 (1999).
[84] S. Shimizu and H. S. Chan, J. Chem. Phys. **113**, 4683 (2000).
[85] N. T. Southall, K. A. Dill, and A. D. J. Haymet, J. Phys. Chem. B **106**, 521 (2002).
[86] M. W. Mahoney and W. L. Jorgensen, J. Chem. Phys. **114**, 363 (2001).
[87] G. Palinkas, I. Bako, K. Heinzinger, and P. Bopp, Mol. Phys. **73**, 897 (1991).
[88] I. M. J. J. van de Ven-Lucassen, T. J. H. Vlugt, A. J. J. van der Zanden, and P. J. A. M. Kerkhof, Mol. Simul. **23**, 79 (1999).
[89] B. J. Palmer, Phys. Rev. E **49**, 359 (1994).
[90] D. Bertolini and A. Tani, Phys. Rev. E **52**, 1699 (1995).
[91] R. Walser, B. Hess, A. E. Mark, and W. F. van Gunsteren, Chem. Phys. Lett. **334**, 337 (2001).
[92] N. G. Fuller and R. L. Rowley, Int. J. Thermophys. **21**, 45 (2000).
[93] D. R. Wheeler and R. L. Rowley, Mol. Phys. **94**, 555 (1998).
[94] J. T. Slusher, Mol. Phys. **98**, 287 (2000).
[95] K. Rah and B. C. Eu, Phys. Rev. E **60**, 4105 (1999).
[96] A. Mukherjee and B. Bagchi, J. Phys. Chem. B **105**, 9581 (2001).
[97] N. Agmon, J. Phys. Chem. **100**, 1072 (1996).
[98] K. Winkler, J. Lindner, H. Bursing, and P. Vohringer, J. Chem. Phys. **113**, 4674 (2000).
[99] H. J. C. Berendsen, J. P. M. Postma, W. F. van Gunsteren, and J. Hermans, in *Intermolecular Forces*, edited by B. Pullman (Reidel, Dordrecht, 1981), pp. 331–342.